DOI: 10.1002/zaac.201300376

On Aliovalent Substitution on the Li Site in $LiMPO_4$: an X-ray Diffraction Study of the Systems $LiMPO_4$–$M_{1.5}PO_4$ (= $Li_xM_{1.5-x/2}PO_4$; M = Ni, Co, Fe, Mn)

Oliver Clemens,*[a][‡] Robert Haberkorn,[b] Michael Springborg,[c] and Horst Philipp Beck[a]

Keywords: $LiFePO_4$; $LiMnPO_4$; $LiCoPO_4$; $LiNiPO_4$; Olivine-type compounds; Aliovalent substitution; Lithium; Phosphorus

Abstract. In this paper we report on the possibility of Li substitution by M^{2+} to various high degrees in $LiMPO_4$ olivine-type compounds (M = Ni, Co, Fe, Mn), depending on the kind of transition metal M. The experimental studies were carried through by reacting stoichiometric amounts of $LiM^{II}PO_4$ and $M^{II}_{1.5}PO_4$ (= $M^{II}_3(PO_4)_2$) to form compounds of composition $Li_xM^{II}_{1.5-x/2}PO_4$ ($0 \le x \le 1$). A complete solid solution over the whole range of x was found for M = Ni (together with a second order structural transition from orthorhombic to monoclinic for decreasing x), whereas far smaller degrees of dopability of the Li site were found for $LiCoPO_4$ and $LiFePO_4$ (up to compositions of approx. $(Li_{0.8}Co_{0.1})CoPO_4$ and approx. $(Li_{0.9}Fe_{0.05})FeO_4$. In addition, the nearly stoichiometric monoclinically distorted olivine-type compounds with compositions $(Li_{0.42-0.47}Co_{0.29-0.265})CoPO_4$ and $(Li_{0.14-0.16}Fe_{0.43-0.42})FePO_4$ could be identified and are described in this article.

Introduction

Olivine-type materials of composition $LiMPO_4$ (M = Ni, Co, Fe, Mn, space group *Pnma*) are promising candidates for cathode materials in lithium ion battery materials.[1] The materials show high voltages (5.1 V for Ni, 4.8 V for Co, 4.1 V for Mn and 3.5 V for Fe[2]) vs. metallic lithium and therefore have high energy storage capacities.

Among those materials, $LiFePO_4$ is by far the most studied compound. Since neither the electronic nor the ionic conductivity of the material is very high, a variety of material modifications have been examined. Among those, reducing the particle size to lower the effective diffusion length of the charge carriers and/or[3] increasing the electronic conductivity by the addition of carbon[4] is mainly used to increase the materials performance.

Many attempts have been made to change the intrinsic properties of $LiFePO_4$, mainly by substitution reactions which change the material composition. Recent reports showed that the incorporation of vanadium into $LiFePO_4$ is beneficial for the material's conductivity.[5] In such synthesis attempts it is hard to determine which crystallographic positions are occupied by the vanadium atoms[5a] and further investigations showed that the material seems to follow a formula of $LiFe_{1-3y/2}V_yPO_4$, incorporating vanadium in its trivalent state, and not a formula $LiFe(PO_4)_y(VO_4)_{1-y}$.[5b] This is in agreement with our earlier observations according to which V^{5+} is not stable in the presence of Fe^{2+}.[6] Nevertheless, $LiMnPO_4$ is tolerant towards doping with vanadium in its highest oxidation state up to a composition of approximately $LiMn(PO_4)_{0.8}(VO_4)_{0.2}$.[7] Such doping increases the electronic conductivity in comparison to $LiMnPO_4$ by one to two orders or magnitudes due to a decrease of the optical band gap.[7]

It has been shown by *Amin* et al. that the ionic conductivity of $LiFePO_4$ can be improved by doping the material with Al^{3+} on the iron site, leading to an overall composition of $Li_{1-y}Fe_{1-y}Al_yPO_4$ [8]. Such substitutions cause the formation of lithium vacancies, which increases the conductivity of the lithium ions along the main conduction pathway along the b-axis.

A lively scientific discussion[9] has followed after an article from *Chung* et al. who claimed to have increased the electronic conductivity of $LiFePO_4$ by doping the material with small amounts of magnesium, niobium, or zirconium on the lithium site.[10] Later investigations showed that this increase in conductivity merely rises from the use of carbon containing pre-

* Dr. O. Clemens
Fax: +49-6151-16 6335
E-Mail: oliver.clemens@nano.tu-darmstadt.de
[a] Universität des Saarlandes
Institut für Anorganische und Analytische Chemie und Radiochemie
Am Markt, Zeile 5
66125 Saarbrücken, Germany
[b] Universität des Saarlandes
Anorganische Festkörperchemie
Am Markt, Zeile 3
66125 Saarbrücken, Germany
[c] Universität des Saarlandes
Physikalische und Theoretische Chemie
Campus B2 2
66123 Saarbrücken, Germany
[‡] Present address: TU Darmstadt
Joint Research Laboratory Nanomaterials
Petersenstraße 32
64287 Darmstadt, Germany
and KIT, Institut für Nanotechnologie
Hermann-von-Helmholtz-Platz 1
76344 Eggenstein-Leopoldshafen, Germany

cursors which help to form highly conductive phases such as carbon, iron phosphides or carbon phosphides on the surface of the grains and therefore improve the overall conductivity.[11] From theoretical calculations the substitution of lithium ions for higher charged cations seems to be unfavorable.[12] $LiFePO_4$ seems to be able to accommodate small amounts of Fe^{2+} on the lithium site ($Li_{0.9}Fe_{1.05}PO_4$)[13] and even the incorporation of higher charged cations (Zr^{4+}, Nb^{5+}, Cr^{3+}) seems to be possible to a small degree (approx. 1 %).[14] $LiNiPO_4$ can be doped on the lithium site by relatively high amounts of Fe^{3+}[15] up to a composition of $Li_{0.55}Fe_{0.15}NiPO_4$. Such reports clearly show that substitution of lithium for higher charged cations is possible in principle. In a recent article, V^{3+} doping on the lithium site was also reported to be possible up to a composition of $Li_{0.7}V_{0.1}FePO_4$.[16] Nevertheless, to the best of our knowledge there have been no experimental studies so far discussing the detailed crystallographic properties that make lithium substitution by higher valent cations feasible for olivine-type compounds.

In this article we report the synthesis of samples of composition $(Li_xM_{0.5-x/2})MPO_4$ (or alternatively written as $Li_xM_{1.5-x/2}PO_4$) ($0 \leq x \leq 1$; M = Ni, Co, Fe), synthesized by high temperature reactions of olivine-type $LiMPO_4$ and the lithium free phosphates of the divalent transition metals $M^{II}{}_{1.5}PO_4$ ($M^{II}{}_3(PO_4)_2$). In addition, we discuss briefly the system with M = Mn. We emphasize that these compositions do not describe a charging/discharging process of a battery process, but describe the aliovalent substitution of Li^+ by the respective transition metal M^{2+} in $LiM^{2+}PO_4$. To clarify the crystal structures discussed in this article, an overview of those under concern is given in section 2. No carbon containing precursors or reductive atmospheres were used in synthesis steps for which samples had to be heated under protective gas atmosphere (M = Fe, Mn) to avoid the formation of impurity phases (as e.g. Fe_2P[10]) which would lead to deviations from the ideal compositions considered in this work. Comparisons of these systems $Li_xM_{1.5-x/2}PO_4$ for the different transition metals M allow for the determination of crystallographic influences which can explain why the degree of substitutability of Li^+ for M^{2+} highly depends on the precise type of M^{2+}.

An Overview of the Crystal Structures Reported for $LiMPO_4$ and $M_{1.5}PO_4$-type Compounds (M = Ni, Co, Fe, (Mn))

The Olivine-type Structure (Triphylite-type) of $LiMPO_4$ (M = Ni, Co, Fe, Mn)

The olivine-type structure (space group *Pnma*) is exemplarily shown for $LiNiPO_4$[17] in Figure 1a. The structure can be understood as a hexagonal close packing of oxygen ions with stacking along the a axis. P^{5+} occupies 1/8 of the tetrahedral sites and Li^+ and Ni^{2+} occupy 1/4 of the octahedral sites in an ordered manner. Characteristic channels of edge-shared LiO_6 octahedra are located along the *c* axis. This direction is reported to have the highest conductivity for Li^+ ions,[12b] although similarly good ionic conductivity might be also found along the c-axis.[18] Edge-sharing is also found between tetrahedra of P^{5+} and octahedra of Ni^{2+} resulting in typical off-center shifts of the cations as expected from Pauling's rules.

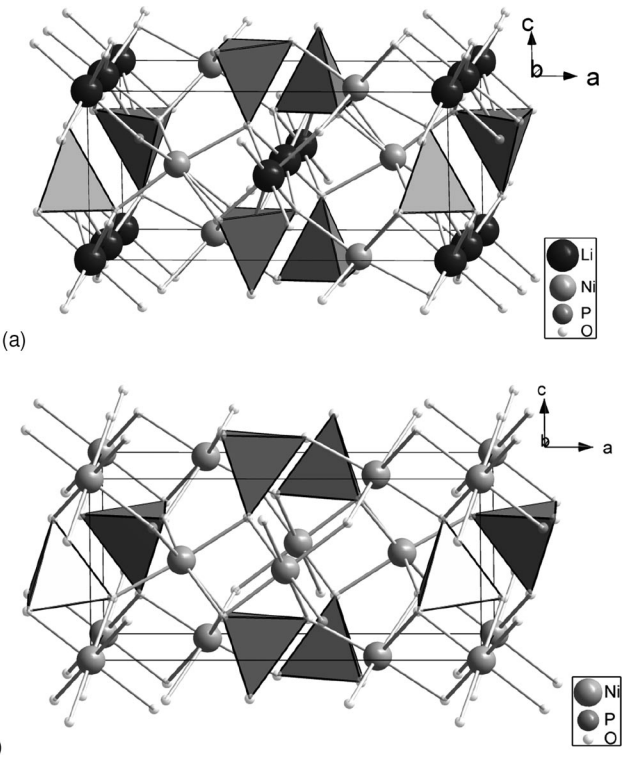

Figure 1. (a) Crystal structure of $LiNiPO_4$ (space group *Pnma*). Phosphorus is located in the solid tetrahedra. (b) Crystal structure of sarcopside-type $Ni_{1.5}PO_4$ in the non-conventional space group setting $P112_1/a$. Again, phosphorus is found in the solid tetrahedra.

The Sarcopside-type Crystal Structure of $Ni_{1.5}PO_4$, the High-pressure Modification of $Fe_{1.5}PO_4$ and a Metastable Modification of $Co_{1.5}PO_4$ (= $M_3(PO_4)_2$)

The crystal structure of $Ni_{1.5}PO_4$ is shown in Figure 1b (space group $P112_1/a$). The structure is related to the olivine-type structure[19] and their relationship can be understood by group–subgroup relationships.[20] $P112_1/a$ is a translationengleiche subgroup (t2) of *Pnma*. A symmetry tree according to the Bärnighausen notation[21] is shown in Figure 2. By this lowering of symmetry, the 4*a* lithium site splits into two sites with multiplicity 2, of which only the 2*a* site is occupied by nickel in $Ni_{1.5}PO_4$. This results in an alternating occupation of the octahedral sites in the channels along the *b*-axis.

This structure exists also for $Co_{1.5}PO_4$ and $Fe_{1.5}PO_4$. The most stable modification of $Fe_{1.5}PO_4$ is the graftonite modification (see section 3.1.3), however the olivine related sarcopside modification can be obtained, too, by a hydrothermal reaction (300 °C, 800 bar, 7 days reaction time).[22] For $Co_{1.5}PO_4$, the sarcopside modification can be obtained through a kind of ion exchange reaction in the melt[23] starting from $LiCoPO_4$ and $CoSO_4$ according to the reaction scheme

$$LiCoPO_4 + CoSO_4 \rightarrow 2\ Co_{1.5}PO_4 + Li_2SO_4$$

and, subsequently, extracting Li_2SO_4 with water.

Zeitschrift für anorganische und allgemeine Chemie ZAAC Journal of Inorganic and General Chemistry

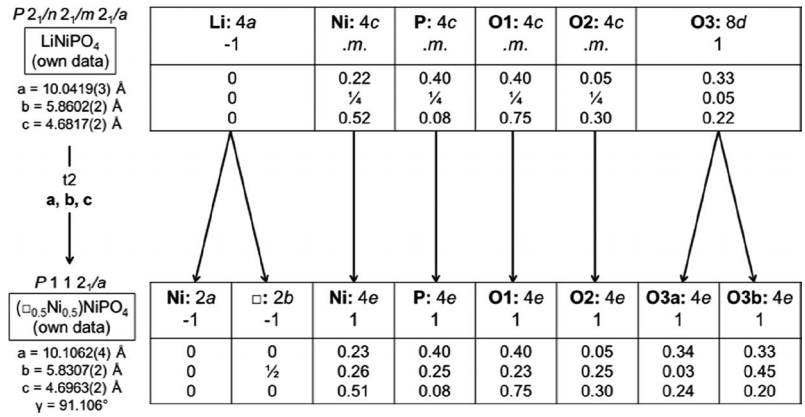

Figure 2. Symmetry tree according to the Bärnighausen notation showing the structure relationship between $LiNiPO_4$ (*Pnma*) and $Ni_{1.5}PO_4$ ($P112_1/a$).

It might be worth mentioning that so far no olivine-related structure has been reported for $Mn_{1.5}PO_4$.

The Crystal Structure of $Co_{1.5}PO_4$

The modification of $Co_{1.5}PO_4$ which is most stable at ambient conditions crystallizes in the monoclinic space group $P2_1/c$[24] (see Figure 3). The structure is not simply related to the olivine-type structure and shows a layer like distribution of Co^{2+} and P^{5+} between highly distorted hexagonal close packed layers of O^{2-}. Co^{2+} can be found in distorted octahedral and distorted trigonal-bipyramidal coordination.

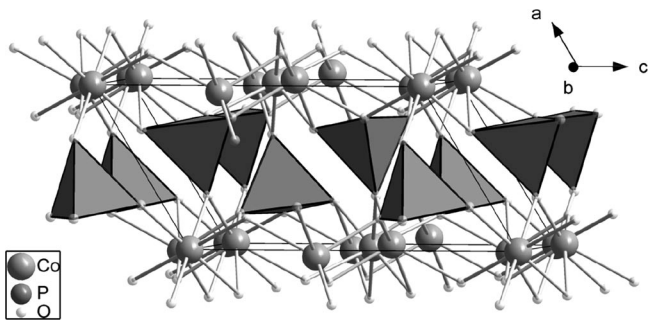

Figure 3. Crystal structure of $Co_{1.5}PO_4$ (space group $P2_1/c$). Phosphorus is located in the solid tetrahedra.

The Crystal Structure of $Fe_{1.5}PO_4$

At ambient conditions, $Fe_{1.5}PO_4$ (graftonite) crystallizes in the monoclinic crystal system with space group $P2_1/c$.[25] A structural drawing is shown in Figure 4. As in the previous subsection, also this structure is not related to the olivine-type structure and can also not be derived from a close packing of O^{2-} ions. Fe^{2+} is located on three different crystallographic sites showing different coordination geometries: distorted octahedral (with one of those Fe–O distances being very large, i.e. approx. 2.68 Å) and trigonal-bipyramidal.

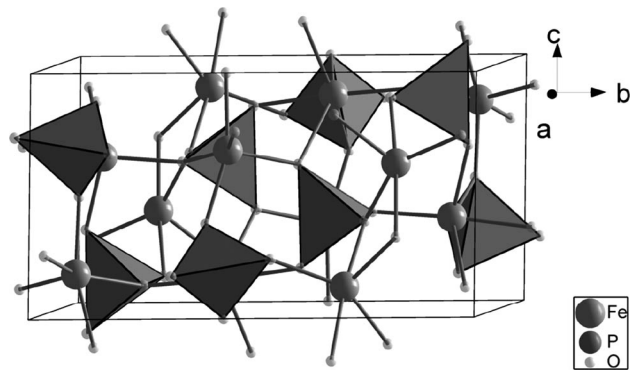

Figure 4. Crystal structure of $Fe_{1.5}PO_4$ (graftonite modification, space group $P12_1/c1$). Phosphorus is located in the solid tetrahedra.

Results and Discussion

Crystallographic Investigations of the Systems $LiMPO_4$–$M_{1.5}PO_4$

$Li_xM_{1.5-x/2}PO_4$ with M = Ni

The synthesis of the compounds of the system $Li_xNi_{1.5-x/2}PO_4$ ($0 \leq x \leq 1$; $\Delta = 0.1$) resulted in the formation of phase-pure products for all compositions under investigation. An overview of the XRD patterns is given in Figure 5, and a Rietveld fit of the XRD pattern of the compound $Li_{0.4}Ni_{1.30}PO_4$ is exemplarily shown in Figure 6. For lithium rich compositions ($0.7 \leq x \leq 1$) we found the compounds to crystallize in the orthorhombic olivine-type structure (space group *Pnma*). Single phase olivine-type compounds were also found for nickel-richer compositions ($0 \leq x < 0.7$), but in addition an increasing monoclinic distortion was found for decreasing x (clearly seen by additional reflections induced by the loss of translational symmetry and additional splitting of reflections). The Rietveld analysis of the XRD patterns of the different compounds showed that only the 2*a* site is occupied by Ni^{2+} for $x < 0.7$, but not the 2*b* site for those monoclinic compounds. However, Li^+ may nevertheless be located on the 2*b* site to some extent but cannot be located by means of X-ray

diffraction due to its weak scattering power. The monoclinic distortion is therefore likely to result from an increase of the number of "Ni^{2+}–Ni^{2+} interactions", which make an ordering of those cations more favourable. The fact that a distinct concentration of nickel cations per unit cell is necessary to give rise to the distortion undermines this assumption.

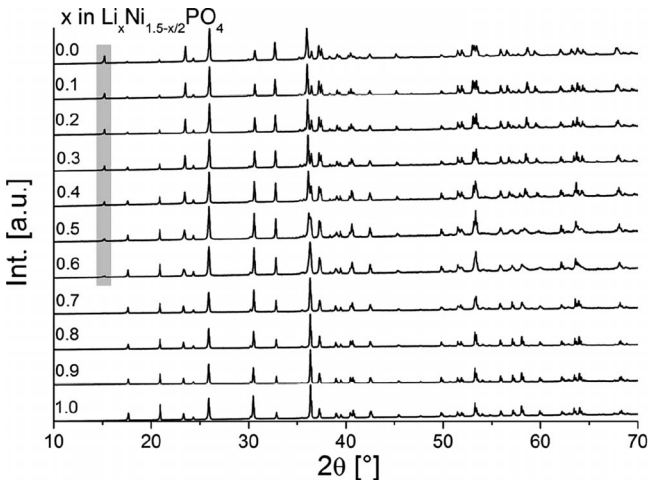

Figure 5. XRD patterns of the compounds with compositions $Li_xNi_{1.5-x/2}PO_4$, all crystallizing in an olivine-type structure. The (0 1 0) reflection appearing due to the monoclinic distortion and the loss of translational symmetry (i.e. the glide mirror plane n) is marked grey.

Additional constraints to a composition of $Li_xNi_{1.5-x/2}PO_4$ were used to allow for the refinement of the composition x of the olivine-type phases. The refined value of x is in very good agreement with the one expected from the amounts of $LiNiPO_4$ and $Ni_{1.5}PO_4$ used for the synthesis, which again supports the consensus that the synthesis of compounds with the formula $Li_xNi_{1.5-x/2}PO_4$ was successful. It might be also worth mentioning that refinements using a monoclinic together with an orthorhombic olivine-type phase for $0.1 \leq x \leq 0.9$ did not result in a proper description of the patterns.

The refined lattice parameters are given in Table 1. Figure 7 depicts the dependencies of the lattice parameters and cell volume on the composition (relative to the values for $LiNiPO_4$). Figure 8 shows the dependency of the angle γ on x in $Li_xNi_{1.5-x/2}PO_4$. The change of lattice parameters is almost linear functions on x, being in good agreement with what is expected for solid solutions according to Vegard's law. The monoclinic angle gamma increases continuously for decreasing values of x for $x < 0.7$. Overall, the lattice shows an expansion when exchanging 2 Li^+ by 1 Ni^{2+}. However the b-axis does not follow this overall trend and shrinks during this substitution process.

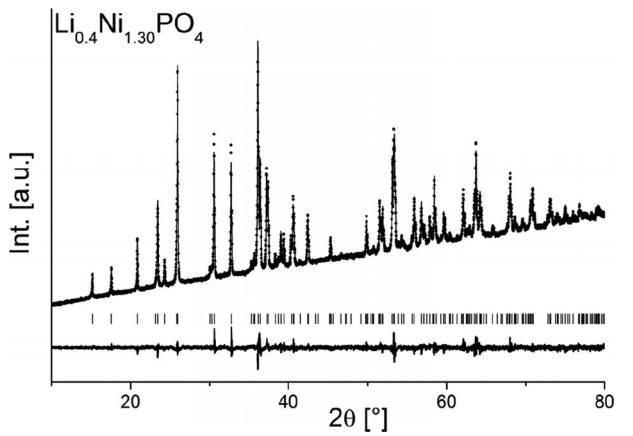

Figure 6. Rietveld analysis of XRD data of the sample of nominal composition $Li_{0.4}Ni_{1.30}PO_4$ (space group $P112_1/a$). The Figure shows the measured (black dots) and the refined intensities (grey line) and the difference curve (black).

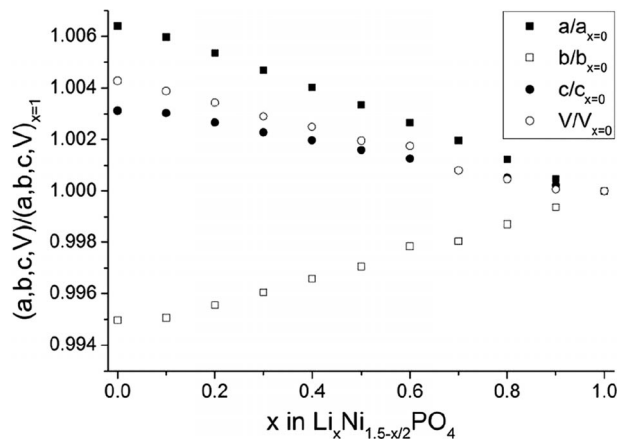

Figure 7. Dependency of lattice parameters and cell volume (normalized to $LiNiPO_4$) on x in $Li_xNi_{1.5-x/2}PO_4$.

Table 1. Refined lattice parameters and lithium content x from a Rietveld analysis of samples of composition $Li_xNi_{1.5-x/2}PO_4$. The standard deviations for the lattice parameters given in this Table are the ones calculated by the Rietveld procedure multiplied by 4.

x in $Li_xNi_{1.5-x/2}PO4$	RG	a /Å	b /Å	c /Å	γ /°	V /Å^3	$x_{refined}$
1	*Pnma*	10.0419(3)	5.8602(2)	4.6817(2)	90	275.50(1)	1
0.9	*Pnma*	10.0467(3)	5.8564(2)	4.6828(2)	90	275.52(1)	0.89(1)
0.8	*Pnma*	10.0544(3)	5.8525(2)	4.6841(2)	90	275.63(1)	0.80(1)
0.7	*Pnma*	10.0617(8)	5.8487(4)	4.6854(4)	90	275.73(3)	0.72(2)
0.6	$P112_1/a$	10.0686(12)	5.8475(8)	4.6876(8)	90.273(8)	275.98(6)	0.62(2)
0.5	$P112_1/a$	10.0756(8)	5.8429(4)	4.6892(4)	90.487(4)	276.05(4)	0.52(2)
0.4	$P112_1/a$	10.0824(4)	5.8401(2)	4.6909(2)	90.656(2)	276.19(2)	0.40(1)
0.3	$P112_1/a$	10.0889(3)	5.8370(2)	4.6923(2)	90.783(2)	276.30(1)	0.30(1)
0.2	$P112_1/a$	10.0957(2)	5.8341(2)	4.6942(2)	90.902(2)	276.45(1)	0.19(1)
0.1	$P112_1/a$	10.1019(3)	5.8312(2)	4.6958(2)	91.016(2)	276.57(1)	0.09(1)
0	$P112_1/a$	10.1062(4)	5.8307(2)	4.6963(2)	91.106(2)	276.68(2)	0

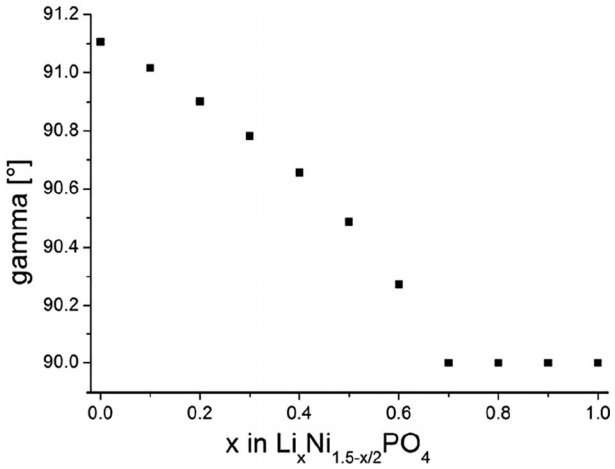

Figure 8. Dependency of the cell parameter γ on x in $Li_xNi_{1.5-x/2}PO_4$. An orthorhombic cell was used for $x \geq 0.7$.

We shall here present a possible reason behind this anisotropic behavior of the b-axis as a function of x. Along this direction channels of edge-sharing Li^+/Ni^{2+} coordination octahedra are found. In $LiNiPO_4$ every octahedron is occupied by Li^+, whereas only every second octahedron is occupied by a Ni^{2+} cation in $Ni_{1.5}PO_4$. One may compare the Coulomb repulsion in a chain of single charged cations with distance d_0

$$\frac{1 \cdot e^2}{4\pi\varepsilon_0 \cdot d_0} \cdot \sum_{i=1}^{2n} i \cdot \frac{1}{2n+1-i}$$

with the Coulomb repulsion in a chain of double charged cations with distance $2d_0$

$$\frac{4 \cdot e^2}{4\pi\varepsilon_0 \cdot 2d_0} \cdot \sum_{i=1}^{n} i \cdot \frac{1}{n+1-i},$$

where e is the elementary charge, ε_0 the dielectric constant of vacuum, and n the number of unit cells included in the summation, describing all possible repulsive interactions. The difference in Coulomb repulsion per mol of $Li_xNi_{1.5}PO_4$ between both models can then be calculated as:

$$\lim_{n\to\infty}\left[\left(2 \cdot \frac{1}{4} \cdot \frac{1}{n} \cdot N_A\right) \frac{e^2}{4\pi\varepsilon_0 \cdot d_0} \cdot \left(\sum_{i=1}^{2n} i \cdot \frac{1}{2n+1-i} - \sum_{i=1}^{n} 2i \cdot \frac{1}{n+1-i}\right)\right]$$

which is approx. 330 kJ·mol^{-1} for $d_0 \approx b/2$. Therefore, the smaller Coulomb repulsion for the Ni-richer compounds can be counterbalanced by a decrease in the distance d_0, i.e. a decrease of the lattice parameter b. This very simple model neglects interactions between the cations in the different channels as well as size effects; however, it can provide a qualitative understanding of the anisotropic expansion behavior of the structure.

Since the precise positions of Li^+ can hardly be located by means of X-ray diffraction, DFT based calculations were used to investigate the compound $Li_{0.5}Ni_{1.25}PO_4$ (whereby the unit cell contains 2 Li^+ and 5 Ni^{2+} ions). The unit cell contains two channels (one at the corners of the cell and one in its center running along the b axis in both cases), where the substitution takes place and where the ions can be distributed on two positions of the same channel. We performed full relaxations of the crystal structure without restrictions on the symmetry and found that it is energetically most favorable that the vacancy is located in the octahedron neighboring the additional Ni^{2+} within the same channel (see Table 2). This is in agreement with results of similar calculations,[12] and the clustering of $Ni^{\bullet}_{Li}$ and V'_{Li} seems to be energetically favorable by about 0.7 eV.

Table 2. Results for cell relaxations and energy calculations of $Li_{0.5}Ni_{1.25}PO_4$ with different distributions of Li^+, Ni^{2+} and vacancy.

position	Setting 1	Setting 2	Setting 3
0, 0, 0 channel along the edge	Li^+	Li^+	empty
0, $^1/_2$, 0 channel along the edge	empty	Li^+	Li^+
$^1/_2$, 0, $^1/_2$ channel along the center of the a/c-plane	Li^+	Ni^{2+}	Li^+
$^1/_2$, $^1/_2$, $^1/_2$ channel along the center of the a/c-plane	Ni^{2+}	empty	Ni^{2+}
volume /Å^3	285.53	282.63	285.91
energy /eV	–173.036	–173.716	–173.041

For monoclinically distorted compounds, nickel was not found to be located (although small traces of an order of some few percent cannot be ruled out) on the 2*b* site. To trace the reasons for this "lack of disorder" we investigated the average M–O distances for the lithium site (4*a* for *Pnma* and 2*a*/2*b* for $P112_1/a$, respectively) and the nickel site (4*c* in *Pnma* and 4*e* in $P112_1/a$), which are depicted in Figure 9. The monoclinic distortion and lowering of symmetry allows for a contraction of the octahedron around 2*a* and an expansion of the octahedron around 2*b*. The average distance around Ni^{2+} on 4*c*/4*f* is not influenced by the substitution process. We suggest that this behavior of the octahedra sizes is favorable for the following reasons:

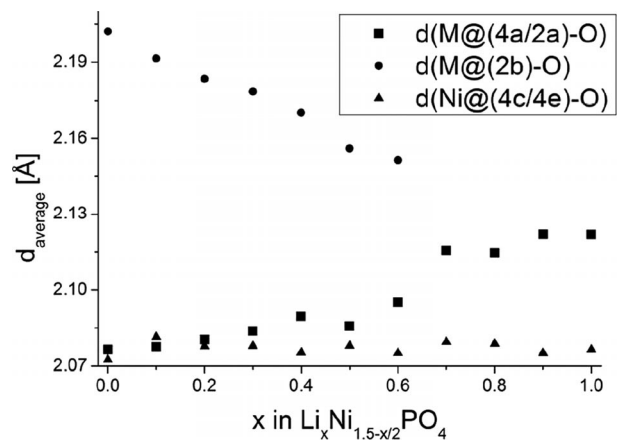

Figure 9. Average M–O distances for the compounds of composition $Li_xNi_{1.5-x/2}PO_4$.

– Ni^{2+} is smaller [26] than Li^+ (ionic radii of 0.69 vs. 0.76 Å for sixfold coordination) and has a higher positive charge, which causes an increasing attractive interaction with the sur-

rounding oxygen ions and therefore contracts the 2*a* octahedron.
– Since the 2*b* position becomes increasingly depopulated for decreasing *x*, an increase in the Coulomb repulsion can then be found for the anions surrounding this site, explaining the expansion of the octahedron around this site.
– Expansion and contraction of octahedra counter balance each other, which can be seen by considering the change in volume. The overall difference in the cell volume between $Ni_{1.5}PO_4$ and $LiNiPO_4$ is only about 0.4 %, showing that there is a relatively good size match between those two compounds, a fact often found necessary for the formation of homogeneous solid solutions.

Our experiments on the $LiNiPO_4$–$Ni_{1.5}PO_4$ system show that aliovalent doping on the lithium site is, in principle, possible. They also demonstrate what an energetically favorable structural relaxation of the lattice could look like. As we shall show below, a comparison with the other systems $LiCoPO_4$–$Co_{1.5}PO_4$ and $LiFePO_4$–$Fe_{1.5}PO_4$ that will be discussed in the following sections will allow for the determination of further influences on the dopability of the lithium site.

$Li_xM_{1.5-x/2}PO_4$ with M = Co

The system $Li_xCo_{1.5-x/2}PO_4$ is distinct from the system $Li_xNi_{1.5-x/2}PO_4$ and does not form single phase solid solutions over the whole range of compositions. The obtained phases together with their relative amount are summarized in Figure 10.

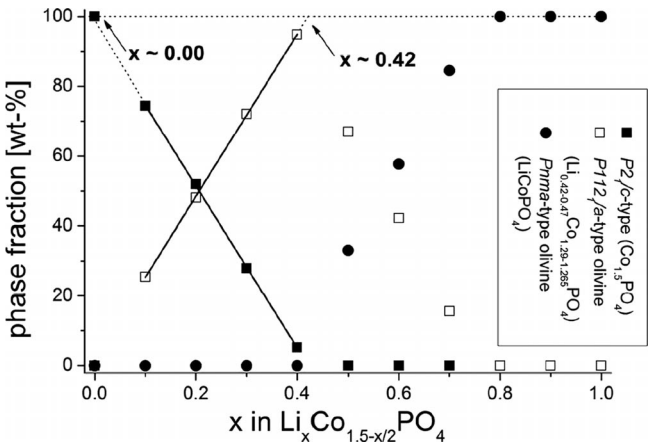

Figure 10. Phases and phase fractions (from a Rietveld analysis) found for different compositions *x* of the system $Li_xCo_{1.5-x/2}PO_4$.

Orthorhombic olivine-type samples can be found for the composition range $0.8 \leq x \leq 1$ (the corresponding diffraction patterns are shown in Figure 11). The distribution of Co^{2+} ions is then likely to be nearly random and no ordering was found in our study. The lattice parameters (see Table 3 and Figure 12) show a Végard like behavior (again with a different behavior of the *b*-axis compared to the other crystallographic directions, although much less pronounced than found for the nickel compounds) and the refined compositions x are in excellent agreement with what would be expected from the amounts of $Co_{1.5}PO_4$ and $LiCoPO_4$ used for synthesis. The increase of volume on Co^{2+} substitution is about 0.4 % (for a step in composition $\Delta x = 0.2$) and therefore far larger than for $Li_xNi_{1.5-x/2}PO_4$, where the same increase of volume was observed for $\Delta x = 1$.

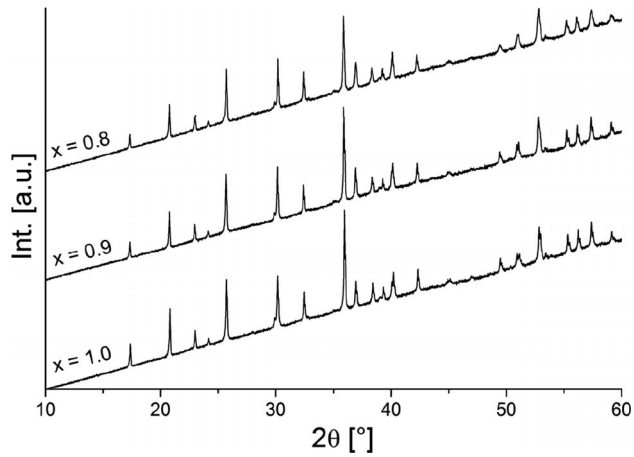

Figure 11. Diffraction patterns for the compounds of composition $Li_xCo_{1.5-x/2}PO_4$. The increase of background results from the high fluorescence of cobalt and the use of a variable divergence slit.

Table 3. Refined lattice parameters and lihtium content *x* from a Rietveld analysis of samples of composition $Li_xCo_{1.5-x/2}PO_4$. The standard deviations for the lattice parameters given in this Table are the ones calculated by the Rietveld procedure multiplied by 4.

x in $Li_xCo_{1.5-x/2}PO_4$	*a* /Å	*b* /Å	*c* /Å	*V* /Å^3	$x_{refined}$
1.0	10.2038(4)	5.9228(4)	4.7002(2)	284.06(3)	1 (fix)
0.9	10.2157(8)	5.9217(4)	4.7053(4)	284.64(3)	0.898(5)
0.8	10.2264(8)	5.9200(4)	4.7087(4)	285.07(4)	0.810(5)

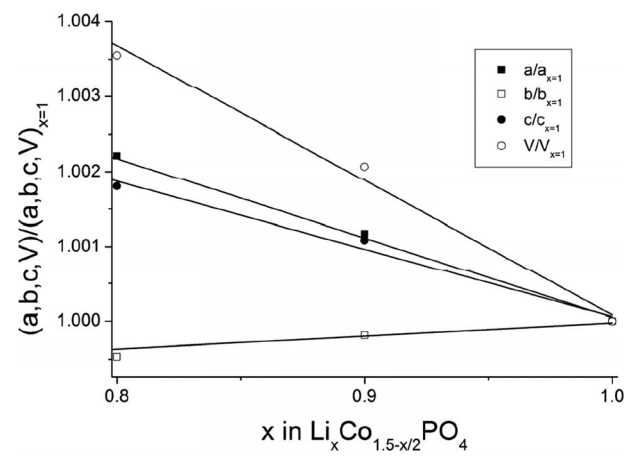

Figure 12. Dependency of lattice parameters on *x* for orthorhombic olivine-type compounds of the system $Li_xCo_{1.5-x/2}PO_4$.

Reducing the lithium content further gives rise to the appearance of a second, monoclinically distorted olivine-type phase. We could determine its composition to be close to $Li_{0.42-0.47}Co_{1.29-1.265}PO_4$ (see later in this section). Such mixtures of an orthorhombic and a monoclinic olivine-type phase

Zeitschrift für anorganische und allgemeine Chemie ZAAC Journal of Inorganic and General Chemistry

were found for compositions with $0.5 \leq x \leq 0.7$. It is worth mentioning that assuming a single monoclinic compound did not result in a proper description of the XRD patterns for this compositional range. During refinement and phase quantification (see also Figure 13) we found no change of the lattice parameters which had been observed for the coexisting boundary phases $Li_{0.8}Co_{1.1}PO_4$ and for $Li_{0.42–0.47}Co_{1.29–1.265}PO_4$ as can be expected for the formation of a two phase mixture.

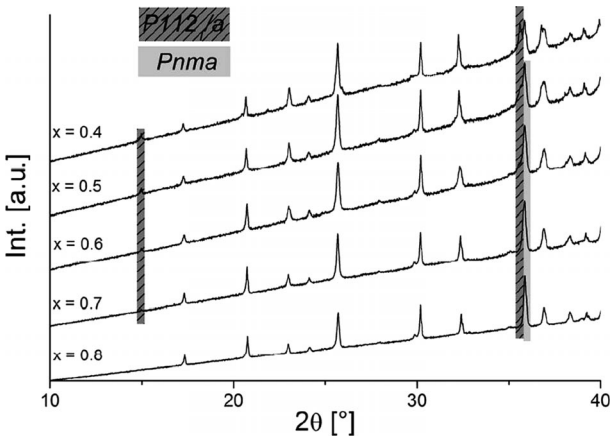

Figure 13. XRD patterns of samples of composition $Li_xCo_{1.5–x/2}PO_4$ ($0.4 \leq x \leq 0.8$). The increase of background results from the high fluorescence of cobalt and the use of a variable divergence slit.

Further decreasing the lithium content again results in the formation of two-phase mixtures. In the composition range of $0.1 \leq x \leq 0.4$ a mixture of monoclinically distorted olivine-type $Li_{0.42–0.47}Co_{1.29–1.265}PO_4$ and a monoclinic non-olivine-type $Co_{1.5}PO_4$ (reported to be stable at ambient conditions, see above) was found. For $x = 0$ single phase non-olivine-type monoclinic $Co_{1.5}PO_4$ was found. The diffraction patterns are presented in Figure 14. The sample with composition $x = 0.4$ allowed for a good structural characterization of the monoclinically distorted olivine-type compound, since no orthorhombic olivine-type compound was present for this composition (although a small amount of approx. 5 wt.-% $Co_{1.5}PO_4$; see Table 4). This structural model was then used without further changes for the refinement of the samples with $0.5 \leq x \leq 0.7$. The Lithium content as obtained from this refinement gives a composition of approximately $Li_{0.47}Co_{1.265}PO_4$, again in excellent agreement with the dependence of the phase quantities found for this system (which indicates a lithium content x of approx. 0.42). This phase can therefore be considered as a new phase in the phase diagram of $Li_2O–CoO–P_2O_5$ and is likely to have a narrow compositional range of stability. The phase is similar to the monoclinically distorted compounds of the system $Li_xNi_{1.5–x/2}PO_4$ in so far that only the 2*a* site is occupied by the transition metal. Again, a contraction of the octahedron around 2*a* was found, whereas that around 2*b* was found to expand. The fact that no change of cell parameters was found for the accompanying $Co_{1.5}PO_4$ phase in preparations in the compositional range $0 < x \leq 0.4$ indicates that the occupancy of interstitial sites by Li^+ might be structurally unfavorable for this compound.

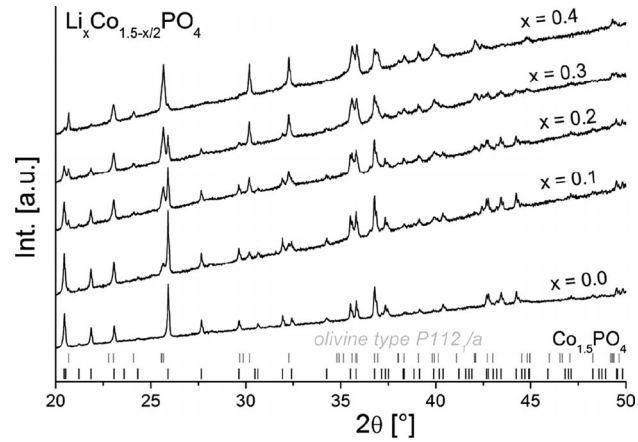

Figure 14. XRD patterns of samples of composition $Li_xCo_{1.5–x/2}PO_4$ ($0 \leq x \leq 0.4$). Bragg markers are shown for monoclinically distorted olivine-type $Li_{0.42–0.47}Co_{1.29–1.265}$ and non-olivine-type $Co_{1.5}PO_4$. The increase of background results from the high fluorescence of cobalt and the use of a variable divergence slit.

Table 4. Structural parameters and average bond lengths of the monoclinically distorted olivine-type compound $Li_{0.47}Co_{1.265}PO_4$ from a Rietveld analysis of the XRD pattern of the sample with composition $Li_{0.4}Co_{1.3}PO_4$ (small amounts of $Co_{1.5}PO_4$ were present in addition). The standard deviations for the lattice parameters given in this Table are the ones calculated by the Rietveld procedure multiplied by 4.

	Refined value
a /Å	10.275(1)
b /Å	5.9173(8)
c /Å	4.7268(8)
γ /°	90.68(1)
V /Å^3	287.38(8)
x	0.470(7)
$\bar{d}$(Co@4*e*–O) /Å	2.12
$\bar{d}$(P@4*e*–O) /Å	1.59
$\bar{d}$(2*a*–O) (Li^+/Co^{2+}) /Å	2.08
$\bar{d}$(2*b*–O) (Li^+/empty) /Å	2.25

A reason for the lack of a complete solid solution range for $0.1<x<0.7$ between the two structurally very similar olivine-type phases might be found in the far larger difference of cell volumes for monoclinically distorted and orthorhombic compounds in the $Li_xCo_{1.5–x/2}PO_4$ system. This will be discussed in more detail below.

$Li_xM_{1.5–x/2}PO_4$ with M = Fe

The system $Li_xFe_{1.5–x/2}PO_4$ is similar to the system $Li_xCo_{1.5–x/2}PO_4$ (see Figure 15 for an overview of the observed phases together with their fractional occurrences for different compositions of $Li_xFe_{1.5–x/2}PO_4$) with a different limit of dopability for the orthorhombic olivine-type phase. Again, a monoclinically distorted olivine-type phase appears which shows a lower lithium content than found for the cobalt system.

For the system $Li_xFe_{1.5–x/2}PO_4$, phase pure orthorhombic olivine-type compounds were only observed for $x \geq 0.9$ (see Figure 16 for the Rietveld fit of the pattern for $Li_{0.9}Fe_{1.05}PO_4$). Interestingly, this is accompanied by an increase of all three

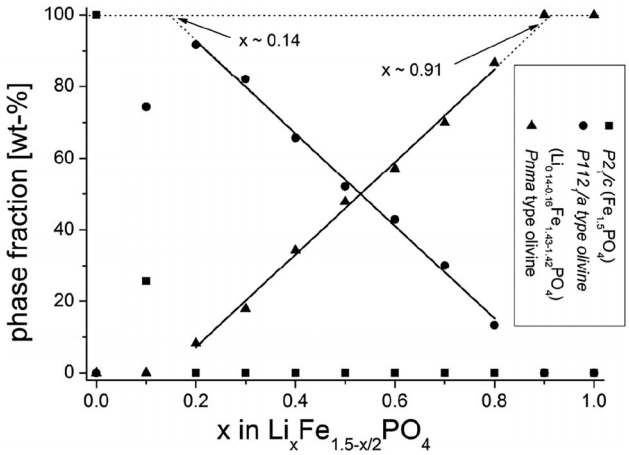

Figure 15. Phases and phase fractions (from a Rietveld analysis) found for different compositions x of the system $Li_xFe_{1.5-x/2}PO_4$.

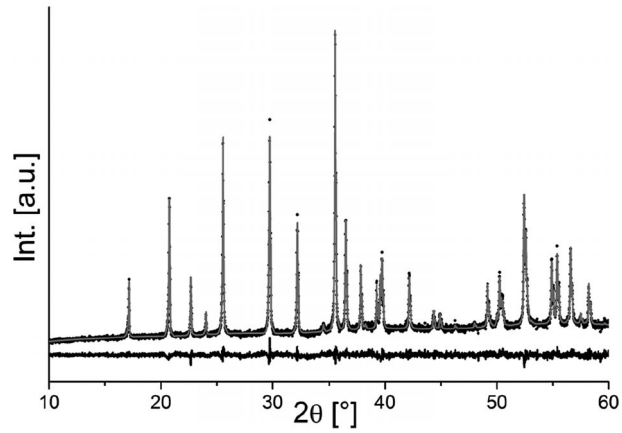

Figure 16. Rietveld analysis of XRD data of the sample of nominal composition $Li_{0.9}Fe_{1.05}PO_4$ (space group $P112_1/a$). The Figure shows the measured (black dots) and the refined intensities (grey line) and the difference curve (black).

crystallographic axes (see refined lattice parameters shown in Table 5), which might indicate that iron is too large for a contraction along b as expected from its higher charge. The refined composition for the sample with $x = 0.9$ was determined to be $Li_{0.89}Fe_{1.055}PO_4$ and is again in excellent agreement with what would have been expected from the amounts of $LiFePO_4$ and $Fe_{1.5}PO_4$ used for synthesis.

Mixtures of this monoclinically distorted olivine-type compound and an orthorhombic olivinetype compound were observed for compositions with $0.2 \leq x \leq 0.8$. From the fact that no further change of the lattice parameters was observed and also from the refined phase fractions shown in Figure 15, we conclude that the minimum value of x which could be stabilized in an orthorhombic olivinetype phase must be close to 0.9 in the $Li_xFe_{1.5-x/2}PO_4$ system. A structural characterization of the monoclinically distorted olivine-type phase was performed on the sample with nominal composition $Li_{0.2}Fe_{1.40}PO_4$ (see Table 6). The structural refinement indicates a molecular formula of $Li_{0.16}Fe_{1.42}PO_4$, again in good agreement with what would be expected from the plot of the weight fractions ($Li_{0.14}Fe_{1.43}PO_4$). As for the example with M = Co and Ni, only the 2*a* site was found to be occupied for the monoclinically distorted compound. Again the same contraction / expansion behavior of the octahedra around 2*a* / 2*b* as for the Ni/Co systems was found (see Table 7).

Table 5. Refined lattice parameters and cell volumes for $LiFePO_4$ and $Li_{0.9}Fe_{1.05}PO_4$. The standard deviations for the lattice parameters given in this Table are the ones calculated by the Rietveld procedure multiplied by 4.

	$LiFePO_4$	$Li_{0.9}Fe_{1.05}PO_4$
a /Å	10.3306(3)	10.3427(4)
b /Å	6.0079(2)	6.0090(2)
c /Å	4.6917(2)	4.7019(2)
V /Å^3	291.92(2)	292.21(2)

Table 7. Average M–O distances found for $Li_{0.14-0.16}Fe_{1.43-1.42}PO_4$.

$\bar{d}$(Fe(@4*e*)–O) /Å	2.16
$\bar{d}$(P(@4*e*)–O) /Å	1.56
$\bar{d}$(2*a*–O) (Li^+/Fe^{2+}) /Å	2.12
$\bar{d}$(2*b*–O) (Li^+/empty) /Å	2.29

For $x = 0.1$, we found in addition to this phase also graftonite-type $Fe_{1.5}PO_4$, again with the observed weight fractions being in good agreement with what would be expected for the composition of the monoclinically distorted olivine-type phase to be $Li_{0.14-0.16}Fe_{1.43-1.42}PO_4$. The lattice parameters of the graftonite-type $Fe_{1.5}PO_4$ were in excellent agreement with the

Table 6. Structural parameters of the monoclinically distorted olivine-type phase with approximate composition $Li_{0.14-0.16}Fe_{1.43-1.42}PO_4$ (from a Rietveld analysis of the XRD pattern of the sample with composition $Li_{0.2}Fe_{1.40}PO_4$). The standard deviations for the lattice parameters given in this table are the ones calculated by the Rietveld procedure multiplied by 4.

site	atom	*x*	*y*	*z*	occupancy	*B* /Å^2
2*a*	Fe^{2+}	0	0	0	0.841(6)	0.40(7)
	Li^+				0.160(3)	0.40(7)
2*b*	Li^+	0	$^1/_2$	0	0.160(3)	0.40(7)
4*e*	Fe^{2+}	0.2168(2)	0.2619(4)	0.5167(6)	1	0.40(7)
4*e*	P^{5+}	0.3975(4)	0.2393(7)	0.0623(8)	1	0.40(7)
4*e*	O^{2-}	0.393(1)	0.227(2)	0.735(1)	1	0.40(7)
4*e*	O^{2-}	0.037(1)	0.245(2)	0.307(1)	1	0.40(7)
4*e*	O^{2-}	0.326(1)	0.429(2)	0.180(2)	1	0.40(7)
4*e*	O^{2-}	0.337(1)	0.034(2)	0.230(2)	1	0.40(7)
$P112_1/a$; a = 10.433(1) Å, b = 6.0276(6) Å, c = 4.7751(6) Å, γ = 90.867(6)°						
R_{wp}		0.83 %	R_{Bragg}	0.37 %	GOF	1.37

Zeitschrift für anorganische und allgemeine Chemie ZAAC Journal of Inorganic and General Chemistry

ones found for the lithium free composition ($x = 0$) which was also the case for those of the monoclinically distorted olivine-type compound for lithium richer compositions.

Furthermore, we would like to comment on results published by *Axmann* et al.[13] who also observed a maximum degree of substitution of $Li_{0.9}Fe_{1.05}PO_4$. They also reported the appearance of a sarcopside-type (monoclinically distorted olivine-type) phase for lithium poorer compositions (they, however, only studied compositions with $x \geq 0.8$), without giving a further characterization of this sarcopside-type phase. They conclude that "*Attention must be then paid in the preparation process of $LiFePO_4$ to avoid deviations from stoichiometry, in particular Li deficiency*".[13] and this might indeed be important for the preparation of $LiFePO_4$ to maintain charge consistency for an industrial process.

As for the cobalt system, no solid solutions were found between structurally very similar orthorhombic and monoclinic olivine-type phases. The reason for this is probably again the larger difference of cell volumes for those compounds.

$Li_xM_{1.5-x/2}PO_4$ with M = Mn – Some Comments

We also investigated the system $Li_xMn_{1.5-x/2}PO_4$, for which a detailed discussion has been presented earlier.[27] The system is far more complicated and contains structurally unknown phases. We failed so far in solving the structure from powder diffraction data; the indexing was successful for one of the phases, indicating lattice parameters of $a = 8.924(1)$ Å, $b = 9.145(1)$ Å, $c = 8.652(1)$ Å, $\beta = 111.633(6)°$ in space group $P2_1/c$ with a maximum amount of this phase found for the sample of nominal composition $Li_{0.2}Mn_{1.40}PO_4$ together with a further, structurally unknown impurity phase. Furthermore different modifications of $Mn_{1.5}PO_4$ appear depending on the value of x. This again shows that lithium can have a structure dictating role, as was also found for other compounds [28]. However, already for $x = 0.9$ we were not able to obtain a single phase composition (unknown impurity phase) and only a very small degree of Mn/Li substitution can be assumed from the observed change of lattice parameters ($x \geq 0.95$). However, since the precise types of the appearing impurity phases were unknown, we are not able to conclude that this substitution corresponds to a solid solution of the type $Li_xMn_{1.5-x/2}PO_4$. Therefore, $LiMnPO_4$ seems to be even more intolerant towards (smaller degrees of) aliovalent substitution of Li^+ by Mn^{2+}.

Discussion

In Table 8, we summarize the phases that we have identified for the different systems $Li_xM_{1.5-x/2}PO_4$ (M = Ni, Co, Fe). From a comparison of the different systems, we tried to address the following two issues:

– Why is there no formation of solid solutions between orthorhombic and monoclinic olivine-type phases in the systems $Li_xFe_{1.5-x/2}PO_4$ and $Li_xCo_{1.5-x/2}PO_4$, although they show high structural similarity?

Table 8. Summary of the different phases found for the systems $Li_xM_{1.5-x/2}PO_4$ (M = Ni, Co, Fe).

x	$Li_xNi_{1.5-x/2}PO_4$	$Li_xCo_{1.5-x/2}PO_4$	$Li_xFe_{1.5-x/2}PO_4$
1	$Li_xNi_{1.5-x/2}PO_4$ olivine-type, (*Pnma*)	$Li_xCo_{1.5-x/2}PO_4$ olivine-type, (*Pnma*)	$Li_xFe_{1.5-x/2}PO_4$ olivine-type, (*Pnma*)
0.9			
0.8			
0.7		(*Pnma*) + ($P112_1/a$)	
0.6	$Li_xNi_{1.5-x/2}PO_4$ olivine-type, ($P112_1/a$)		
0.5			
0.47-0.42		$Li_{0.47-0.42}Co_{1.265-1.29}PO_4$ olivine-type, ($P112_1/a$)	(*Pnma*) + ($P112_1/a$)
0.4		($P112_1/a$) + ($P2_1/c$)	
0.3			
0.2			
0.16-0.14			$Li_{0.16-0.14}Fe_{1.43-1.42}PO_4$ olivine-type, ($P112_1/a$)
0.1			($P112_1/a$) + ($P2_1/c$)
0		$Co_{1.5}PO_4$ ($P2_1/c$)	$Fe_{1.5}PO_4$ ($P2_1/c$)

– What causes the lower degrees of lithium site doping in the orthorhombic compounds when going from Ni → Co → Fe → Mn?

For the monoclinically distorted olivine-type compounds, one can obtain some information by comparing the unit cell volumes and the volume differences of the respective compounds $LiMPO_4$, olivine-type $M_{1.5}PO_4$ and the monoclinically distorted $Li_xM_{1.5-x/2}PO_4$ olivinetype phases ($x = 0.42$–0.47 for M = Co and $x = 0.14$–0.16 for M = Fe; see Table 9). For the nickel system, the volumes of $LiNiPO_4$ and $Ni_{1.5}PO_4$ differ only by about 1.2 Å^3, whereas for M = Co and Fe this difference is significantly larger (6.4 and 10.1 Å^3). It is well-known that similar atomic sizes are crucial for the formation of solid solutions and the larger volume differences might explain why the formation of a complete solid solution is only possible for M = Ni. The volumes of the monoclinically distorted olivine-type phases lie between those that are found for $LiMPO_4$ and $M_{1.5}PO_4$ (M = Co, Fe) and also in this case the corresponding volume differences again match the composition that was assumed from the structural analysis and phase quantification.

Table 9. Volumes and differences in volume of different compounds of the system $Li_xM_{1.5-x/2}PO_4$. The volume of metastable olivine-type phases reported in literature are given for $Fe_{1.5}PO_4$ and $Co_{1.5}PO_4$. The standard deviations are smaller than number of digits given in this Table.

Volume /Å^3	M = Ni	M = Co	M = Fe
LiMPO4	275.5	284.1	291.2
$M_{1.5}PO_4$	276.7	290.5[23]	301.3[30]
$\Delta(M_{1.5}PO_4–LiMPO_4)$	1.2	6.4	10.1
$Li_xM_{1.5-x/2}PO_4$	–	287.4	300.3
		x ≈ 0.47–0.42	x ≈ 0.16–0.14
$\Delta(M_{1.5}PO_4–Li_xM_{1.5-x/2}PO_4)$	–	3.1	1.0
$\Delta(Li_xM_{1.5-x/2}PO_4–LiMPO_4)$	–	3.4	9.1

Hypothetically, one might suggest the formation of the most stable $M_{1.5}PO_4$ polymorph in addition to an orthorhombic olivine-type phase for $0 < x << 1$ for the systems with M = Co, Fe. The fact that this cannot be observed and that monoclinic olivine-type compounds are formed instead can be understood in terms that the olivine-type structure seems to allow for a distinct degree of configurational entropy, which might be favorable at the temperatures used for synthesis. The occupation of interstitial sites in $Co_{1.5}PO_4$ and $Fe_{1.5}PO_4$ might be energetically costly and the monoclinic olivinetype compounds with

"fine-tuned" composition might be an energetically favorable alternative. In support of this we mention that such a structure determining influence of Li^+ is known in literature,[28] and can be used in rationalizing e.g. the formation and stabilization of the high temperature modification of $Mn_{1.5}VO_4$ by substituting Mn^{2+} for small amounts of Li^+ (or Na^+).[29]

Based on our results of the previous sections, one can predict what a structurally favorable substitution of the lithium site in $LiMPO_4$ would look like. The DFT-based calculations showed that the vacancy is most likely to be located inside an octahedron next to the M^{2+} ion that was incorporated on the lithium site. For $Li_xNi_{1.5-x/2}PO_4$, we found that a contraction of the octahedron around M^{2+} together with an expansion around the vacancy due to increased anion repulsion is energetically favorable. The average distances to the oxide ions of the lithium and M sites for the $LiMPO_4$ compounds are listed in Table 10. It can be seen that nickel and cobalt seem to be remarkably smaller than Li^+, therefore allowing for such an expansion/contraction, i.e. a local relaxation around a defect. For Fe^{2+} the average distances become very similar, resulting in an even lower degrees of substitution. Mn^{2+} seems to be significantly larger than the Li^+ ion, whereby an expansion around Mn^{2+} and the vacancy would have to occur simultaneously, which can explain why the lithium site substitution seems to be highly unfavorable for this compound.

Table 10. Refined average M–O distances for the compounds $LiMPO_4$. The ionic radius of Li^+ according to *Shannon*[26] is 0.76 Å.

M in $LiMPO_4$	$\bar{d}$(Li–O) /Å	$\bar{d}$(M–O) /Å	$r(M)_{Shannon}$ /Å[26]
Ni	2.12	2.08	0.69
Co	2.15	2.10	0.745
Fe	2.15	2.14	0.78
Mn	2.17	2.19	0.83

Conclusions

In this work we have shown that lithium site substitution, even to very high degrees, can be made possible in the potential cathode materials $LiMPO_4$. However, simple geometrical and size relationships can play an important role for the extent to which the ions on the lithium site can be replaced by M^{2+}. Different structural relaxations can occur, and we showed that the investigation of compositions for which multiphase mixtures are obtained can give important information on doping limits and the kind of structural relaxations. This work also has led to the discovery of the two new monoclinically distorted olivine-type compounds $Li_{0.42-0.47}Co_{1.29-1.265}PO_4$ and $Li_{0.14-0.16}Fe_{1.43-1.42}PO_4$.

Experimental Section

Sample Preparation

$LiNiPO_4$ and $Ni_{1.5}PO_4$ were made by heating appropriate stoichiometric amounts of Li_2CO_3 (99 %+, Aldrich), NiO (99.995 %, Kristallhandel Kelpin) and $(NH_4)_2HPO_4$ (p. a., Merck) to 950 °C for 60 h in platinum crucibles in air (twice with one intermediate regrinding), where the precursors were ground by use of a planetary ball mill (Fritsch pulverisette 7, 1 h, approx. 350 rpm). Samples of composition $Li_xNi_{1.5-x/2}PO_4$ ($0.1 \leq x \leq 0.9$; in steps of $\Delta x = 0.1$) were prepared by mixing stoichiometric amounts of $LiNiPO_4$ and $Ni_{1.5}PO_4$ and applying similar synthesis conditions.

$LiCoPO_4$ and $Co_{1.5}PO_4$ were made by twice heating appropriate stoichiometric amounts of Li_2CO_3 (99 %+, Aldrich), CoO (made by heating Co_3O_4 (pure, Merck) at 1250 °C under vacuum) and $(NH_4)_2HPO_4$ (p. a., Merck) to 900 °C for 50 h in a dry flowing argon atmosphere. Grinding of the precursors was again done by use of a planetary ball mill (Fritsch pulverisette 7, 1 h, approx. 350 rpm). Samples of composition $Li_xCo_{1.5-x/2}PO_4$ ($0.1 \leq x \leq 0.9$; in steps of $\Delta x = 0.1$) were prepared by mixing stoichiometric amounts of $LiCoPO_4$ and $Co_{1.5}PO_4$ and applying similar synthesis conditions.

For the preparation of $LiFePO_4$ and $Fe_{1.5}PO_4$, a different approach was used. $FePO_4$ was first synthesized by heating stoichiometric amounts of $FeC_2O_4*2H_2O$ (99 %+, Riedel-de Haen) and $(NH_4)_2HPO_4$ (p. a., Merck) to 900 °C for 60 h in air, applying a slow heating up procedure over 10 h. $FePO_4$ was then mixed with stoichiometric amounts of metallic iron (99 %+, Merck) and heated to 800 °C for 15 h under flowing argon (purity 99.996 % for all the reactions). To avoid oxidation by impurities of oxygen a boat filled with MnO was placed in front of the reaction mixture and the ball milled powders (Fritsch pulverisette 7, 1 h, approx. 350 rpm) were pressed into a tablet to minimize the contact area between the gas and the sample. Samples of compositions $Li_xFe_{1.5-x/2}PO_4$ ($0.1 \leq x \leq 1$; $\Delta x = 0.1$) were prepared by mixing stoichiometric amounts of Li_3PO_4 and $Fe_{1.5}PO_4$ by ball milling the mixtures (Fritsch pulverisette 7, 1 h, approx. 350 rpm) and heating them under similar conditions as for the preparation of $Fe_{1.5}PO_4$.

$LiMnPO_4$ was synthesized by heating stoichiometric amounts of LiH_2PO_4 (99 %+, Aldrich) and MnO (99 %, Alfa Aesar) to 300 °C for 1h and then to 900 °C for 15 h under argon (twice with one intermediate regrinding), where preparation was done by use of a ball mill (Fritsch pulverisette 7, 1 h, approx. 350 rpm). Again, the sample was pressed into a tablet and a boat with MnO was placed in front of the reaction mixture to avoid oxidation by traces of oxygen. $Mn_{1.5}PO_4$ was made by preparing and heating stoichiometric amounts of MnO (99 %, Alfa Aesar) and $(NH_4)_2HPO_4$ (p. a., Merck) under the same conditions as used for the preparation of $LiMnPO_4$. Samples of composition $Li_xMn_{1.5-x/2}PO_4$ ($0.1 \leq x \leq 0.9$; $\Delta x = 0.1$) were then prepared by mixing stoichiometric amounts of $LiMnPO_4$ and $Mn_{1.5}PO_4$ and applying the same synthesis conditions.

According to our experience, the chosen temperature treatments do not cause any loss of lithium and even further treatment at the maximal chosen temperature does not result in any changes of the refined sample composition and determined lattice parameters.

Diffraction Experiments

XRD patterns were recorded with a Panalytical Philips X'Pert Pro diffractometer with focusing Bragg–Brentano geometry and a fine focus X-ray tube with copper anode in a 2θ-range from 10 to 140 degrees. No primary beam monochromator was attached. A fast PIXcel detector and a variable divergence slit were used. The total scan time was 4 hours.

The whole 2θ-range was used for Rietveld analysis by the program TOPAS 4.2[31] (Bruker AXS, Karlsruhe, Germany). The instrumental

Zeitschrift für anorganische und allgemeine Chemie ZAAC Journal of Inorganic and General Chemistry

intensity distribution and peak shape parameters were determined empirically according to the fundamental parameters set[32] after a reference scan of LaB_6. Positional parameters, microstructural and lattice parameters were refined during Rietveld analysis. To refine microstructural parameters, the program TOPAS[31] uses a double Voigt model. The thermal displacement parameters of all atoms of all phases were constraint to an overall B-value to avoid quantification errors. For all olivine-type compounds (orthorhombic or monoclinic) the compositions of the phases were constrained to a formula $Li_xM_{1.5-x/2}PO_4$. No compositions were refined for non-olivine-type compounds since no deviation of lattice parameters was observed in those cases). Based on our experience, the standard deviations for the lattice parameters given in this article are the ones calculated by the Rietveld procedure multiplied by 4.

Quantum Mechanical Calculations

Quantum mechanical calculations were performed using the PAW/GGA+U method as implemented in the program VASP 4.6.[33] The calculations were based on the use of pseudopotentials and of plane waves as basis functions. The cut-off energy of the latter was set equal to 500 eV. As criterion for convergence we required that the total energy was converged to within 0.0001 eV and the forces acting on the atoms were smaller than 0.001 eV $Å^{-3}$. The functional of *Perdew* and *Wang* was used to describe the effects of exchange and correlation[34] and values of $U = 6$ eV and $J = 1$ eV [35] were used to correct Coulomb and exchange interactions for the nickel atoms. These values for U and J are typical for this element.[2] All calculations were spin-polarized and a ferromagnetic configuration for the nickel atoms was initially assumed to reduce the computational costs which arise when using larger supercells. The set of k-points used in k-space sampling was calculated automatically and Γ-centered (75 k-points in total). Such calculations were performed for olivine-type $Li_{0.5}Ni_{1.25}PO_4$, for which different distributions of lithium and nickel atoms were examined.

Acknowledgments

Oliver Clemens thanks the Landesgraduiertenförderung Saarland for financial support.

References

[1] A. K. Padhi, K. S. Nanjundaswamy, J. B. Goodenough, *J. Electrochem. Soc.* **1997**, *144*, 1188–1194.
[2] F. Zhou, M. Cococcioni, K. Kang, G. Ceder, *Electrochem. Commun.* **2004**, *6*, 1144–1148.
[3] a) K. Dokko, S. Koizumi, H. Nakano, K. Kanamura, *J. Mater. Chem.* **2007**, *17*, 4803–4810; b) A. Yamada, S. C. Chung, K. Hinokuma, *J. Electrochem. Soc.* **2001**, *148*, A224–A229.
[4] A. Yamada, M. Yonemura, Y. Takei, N. Sonoyama, R. Kanno, *Electrochem. Solid-State Lett.* **2005**, *8*, A55–A58.
[5] a) J. Hong, C. S. Wang, X. Chen, S. Upreti, M. S. Whittingham, *Electrochem. Solid-State Lett.* **2009**, *12*, A33–A38; b) F. Omenya, N. A. Chernova, S. Upreti, P. Y. Zavalij, K.- W. Nam, X.-Q. Yang, M. S. Whittingham, *Chem. Mater.* **2011**, *23*, 4733–4740.
[6] O. Clemens, M. Bauer, R. Haberkorn, H. P. Beck, *Z. Anorg. Allg. Chem.* **2011**, *637*, 1036–1044.
[7] O. Clemens, M. Bauer, R. Haberkorn, M. Springborg, H. P. Beck, *Chem. Mater.* **2012**, *24*, 4717–4724.
[8] a) R. Amin, C. Lin, J. Maier, *Phys. Chem. Chem. Phys.* **2008**, *10*, 3519–3523; b) R. Amin, C. Lin, J. Maier, *Phys. Chem. Chem. Phys.* **2008**, *10*, 3524–3529.
[9] a) B. L. Ellis, M. Wagemaker, F. M. Mulder, L. F. Nazar, *Adv. Funct. Mater.* **2010**, *20*, 186–188; b) N. Meethong, Y.-H. Kao, S. A. Speakman, Y.-M. Chiang, *Adv. Funct. Mater.* **2009**, *19*, 1060–1070.
[10] S.-Y. Chung, J. T. Bloking, Y.-M. Chiang, *Nat. Mater.* **2002**, *1*, 123–128.
[11] a) N. Ravet, A. Abouimrane, M. Armand, *Nat. Mater.* **2003**, *2*, 702–702; b) P. S. Herle, B. Ellis, N. Coombs, L. F. Nazar, *Nat. Mater.* **2004**, *3*, 147–152.
[12] a) C. A. J. Fisher, V. M. Hart Prieto, M. S. Islam, *Chem. Mater.* **2008**, *20*, 5907–5915; b) M. S. Islam, D. J. Driscoll, C. A. J. Fisher, P. R. Slater, *Chem. Mater.* **2005**, *17*, 5085–5092.
[13] P. Axmann, C. Stinner, M. Wohlfahrt-Mehrens, A. Mauger, F. Gendron, C. M. Julien, *Chem. Mater.* **2009**, *21*, 1636–1644.
[14] M. Wagemaker, B. L. Ellis, D. Lützenkirchen-Hecht, F. M. Mulder, L. F. Nazar, *Chem. Mater.* **2008**, *20*, 6313–6315.
[15] A. Goni, L. Lezama, M. I. Arriortua, G. E. Barberis, T. Rojo, *J. Mater. Chem.* **2000**, *10*, 423–428.
[16] F. Omenya, N. A. Chernova, Q. Wang, R. Zhang, M. S. Whittingham, *Chem. Mater.* **2013**, *25*, 2691–2699.
[17] A. Goñi, L. Lezama, G. E. Barberis, J. L. Pizarro, M. I. Arriortua, T. Rojo, *J. Magn. Magn. Mater.* **1996**, *164*, 251–255.
[18] R. Amin, J. Maier, P. Balaya, D. P. Chen, C. T. Lin, *Solid State Ionics* **2008**, *179*, 1683–1687.
[19] A. G. Nord, *Z. Kristallogr.* **1984**, *166*, 159–176.
[20] H. Bärnighausen, *Match* **1980**, *9*, 139–175.
[21] U. Müller, *Anorganische Strukturchemie*, B. G. Teubner Verlag, Wiesbaden, **2004**.
[22] J. K. Warner, A. K. Cheetham, A. G. Nord, R. B. Von Dreele, M. Yethiraj, *J. Mater. Chem.* **1992**, *2*, 191–196.
[23] G. Berthet, J. C. Joubert, E. F. Bertaut, *Z. Kristallogr.* **1972**, *136*, 98–105.
[24] J. B. Anderson, E. Kostiner, M. C. Miller, J. R. Rea, *J. Solid State Chem.* **1975**, *14*, 372–377.
[25] E. Kostiner, J. R. Rea, *Inorg. Chem.* **1974**, *13*, 2876–2880.
[26] R. D. Shannon, *Acta Crystallogr., Sect. A* **1976**, *32*, 751–767.
[27] O. Clemens, Dissertation Thesis, Universität des Saarlandes (Saarbrücken, http://scidok.sulb.uni-saarland.de/volltexte/2012/4718/), **2011**.
[28] S. Solodovnikov, E. Khaikina, Z. Solodovnikova, *J. Struct. Chem.* **2009**, *50*, 78–85.
[29] a) O. Clemens, R. Haberkorn, H. P. Beck, *J. Solid State Chem.* **2011**, *184*, 2640–2647; b) O. Clemens, R. Haberkorn, M. Springborg, H. P. Beck, *J. Solid State Chem.* **2012**, *194*, 409–415; c) O. Clemens, A. J. Wright, K. S. Knight, P. R. Slater, *Dalton Trans.* **2013**, *42*, 7894–7900.
[30] T. Ericsson, A. G. Nord, *Am. Mineral.* **1984**, *69*, 889–895.
[31] *Topas V4.2*, General profile and structure analysis software for powder diffraction data, User's Manual, Bruker AXS, Karlsruhe, **2008**.
[32] R. W. Cheary, A. A. Coelho, J. P. Cline, *J. Res. Nat. Inst. Stand. Technol.* **2004**, *109*, 1–25.
[33] G. Kresse, J. Furthmüller, *Comput. Mater. Sci.* **1996**, *6*, 15.
[34] J. P. Perdew, Y. Wang, *Phys. Rev. B* **1992**, *45*, 13244–13249.
[35] A. I. Liechtenstein, V. I. Anisimov, J. Zaanen, *Phys. Rev. B* **1995**, *52*, R5467.

Received: July 30, 2013
Published Online: October 15, 2013

